

How much laser power can propagate through fusion plasma?

Pavel M. Lushnikov^{1,2,3} and Harvey A. Rose³

¹ *Landau Institute for Theoretical Physics,
Kosygin St. 2, Moscow, 119334, Russia*

² *Department of Mathematics, University of Notre Dame, Indiana 46556, USA*

³ *Theoretical Division, Los Alamos National Laboratory,
MS-B213, Los Alamos, New Mexico, 87545, USA **

(Dated: August 13, 2018)

Abstract

Propagation of intense laser beams is crucial for inertial confinement fusion, which requires precise beam control to achieve the compression and heating necessary to ignite the fusion reaction. The National Ignition Facility (NIF), where fusion will be attempted, is now under construction. Control of intense beam propagation may be ruined by laser beam self-focusing. We have identified the maximum laser beam power that can propagate through fusion plasma without significant self-focusing and have found excellent agreement with recent experimental data, and suggest a way to increase that maximum by appropriate choice of plasma composition with implication for NIF designs. Our theory also leads to the prediction of anti-correlation between beam spray and backscatter and suggests the indirect control of backscatter through manipulation of plasma ionization state or acoustic damping.

PACS numbers: 42.65.Jx 52.38.Hb

INTRODUCTION

Propagation of intense laser beams in plasma raises outstanding technological and scientific issues. These issues are closely tied with inertial confinement fusion (ICF) [1, 2, 3, 4] which requires precise beam control in order to maintain symmetry of spherical target implosion, and so achieve the compression and heating necessary to ignite the fusion reaction. ICF will be attempted at the National Ignition Facility (NIF). While most engineering features of NIF are now fixed, there are still crucial choices to be made [4] in target designs. Control of intense beam propagation is endangered by laser beam self-focusing, when a beam digs a cavity in plasma, trapping itself, leading to higher beam intensity, a deeper cavity, and so on.

Self-focusing occurs when an intense laser beam propagates through a wide range of optical media [5], and has been the subject of research for more than forty years, since the advent of lasers [6]. In laser fusion the intensity of laser beams is so large that self-focusing in plasma can cause disintegration of a laser beam into many small beams, leading to rapid change in beam angular divergence $\Delta\theta$, called beam spray. Significant beam spray is absolutely unacceptable for attaining fusion which requires precise laser beam control [4]. It was commonly assumed that the main source of beam spray in fusion plasma is the self-focusing in local maxima of laser intensity (hot spots) which are randomly distributed throughout the plasma [4]. Hot spot self-focusing can be controlled by reducing beam correlation time, T_c . However we show in this Article that the main limitation of maximum beam power, which can propagate in plasma without significant beam spray, is determined by collective instability which couples the beam to an ion acoustic wave. We call this instability *collective* forward stimulated Brillouin scatter (CFSBS) [7] because it does not depend on the dynamics of isolated hot spots, but rather the intensity fluctuations as temporally smoothed (averaged) by ion inertia. We show below that this collective instability is consistent with the first experimental observation of the beam spray onset [8] while hot spot self-focusing is not.

BEAM COLLAPSE (CATASTROPHIC SELF-FOCUSING)

There are two self-focusing mechanisms in plasma: ponderomotive and thermal. Historically, ponderomotive self-focusing was studied first. The ponderomotive mechanism results from averaging over fast electron oscillations in the laser electromagnetic field, at frequency ω_0 . Averaging induces an effective electrostatic potential proportional to the local laser intensity, which in turn adds to the usual fluid pressure term in hydrodynamical equations [9]. The thermal mechanism results from the transport of electron temperature fluctuations, δT_e .

Ponderomotive self-focusing in three dimensions (3D) is quite different than in two dimensions (2D). (Here one dimension is the direction of propagation of laser beam with one/two transverse dimensions in 2D/3D, respectively). In 2D, self-focusing often results in propagation of optical pulses (called solitons [10]) without change of their shape over large distances. In 3D, self-focusing often leads to dramatic intensity amplification with propagation distance. Indeed, self-focusing of light, as described by the nonlinear Schrodinger equation, results in formation of a point singularity after finite distance of light propagation [11, 12]. A finite amount of optical power is drawn into this point, usually referred to as beam collapse. Near singularity, the nonlinear Schrodinger equation loses its applicability because of finite density depletion effects and instead of singularity, light scatters in a wide range of angles, causing loss of precise irradiation symmetry necessary for fusion. For application to fusion, only the 3D regime is relevant, and only this regime is considered in this Article. Note that in some regimes other, high frequency instabilities, such as stimulated Raman scatter can also arrest catastrophic collapse (see e.g. Ref. [13]) but they are not considered here.

Beam collapse occurs if the laser beam power, P , exceeds a critical value [12], $P_c \propto T_e/n_e$. T_e and n_e are the electron temperature and density, respectively. For NIF parameters ($n_e \approx 10^{21}/cm^3$, $T_e \approx 5keV$, $\omega_0 \approx 5 \times 10^{15}sec^{-1}$) $P_c = 1.6 \times 10^9$ Watts. This power evaluation is based on Ref. [12], in contrast to threshold given by Max [14], which is roughly half as large. The former may be dynamically realized (see Eq. (107) of Ref. [15]) from non-equilibrium initial conditions, appropriate to initiation by hot spots, while the latter is strictly an equilibrium property, and hence not useful for quantitative beam propagation prediction.

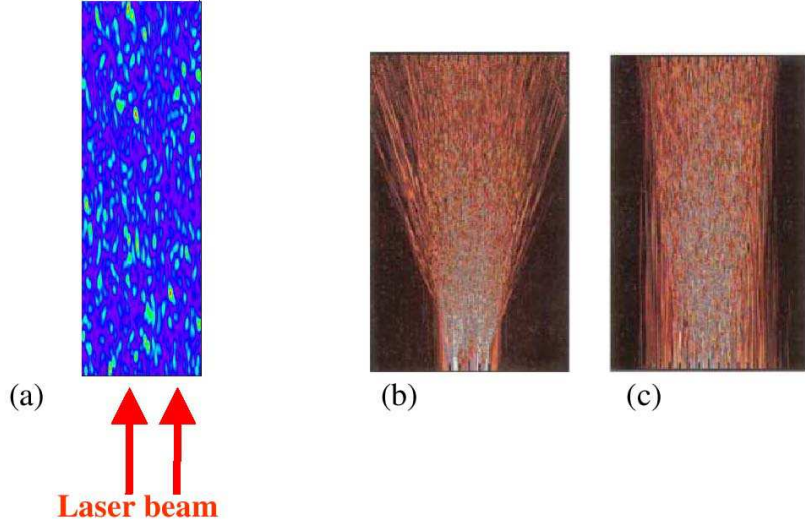


FIG. 1: Figure 1. Two dimensional slice of light intensity fluctuations inside plasma. Laser beam propagates from bottom of figure upward. (a) Distribution of fluctuations at scale much smaller than the beam diameter. Random fluctuations (“speckles”), are highly anisotropic, with correlation or speckle length along the beam propagation, “ z ”, direction about $7F^2\lambda_0$. (b) Beam spray regime of laser propagation. Beam disintegrates into many small beams. (c) Negligible beam spray regime. This regime is necessary for attaining fusion (from Ref. [2] with permission). Horizontal scale in (b) and (c) correspond to beam diameter.

The energy required for inertial confinement fusion is so large that the power in each of NIF’s 48 beam quads [4] exceeds P_c by several orders of magnitude: the power of each NIF beam is approximately 8×10^{12} Watts, or about 5×10^3 critical power. This difficulty is alleviated by the Random Phase Plate (RPP) [16] which splits the laser beam into many (tens of thousands) small beams with random phases, which are then optically focused into plasma (see Figure 2 in Ref. [2]). As a result the total laser beam electric field amplitude, E , is well approximated in vacuum as an anisotropic random Gaussian field, with correlation length l_c perpendicular to the beam propagation direction, much smaller than the parallel correlation length. The laser intensity, $I \propto |E|^2$, forms a speckle field - a random in space distribution of intensity (see Figure 1a).

TIME-INDEPENDENT SELF-FOCUSING

First consider the regime where laser beam time dependence is negligible. If the average intensity, $\langle I \rangle$, is small, then collapse events occur only in speckles (also referred to as hot spots) with $I \gg \langle I \rangle$, so that their power, $P \sim I^2 l_c^2$, exceeds P_c . The width of these intense speckles, $F\lambda_0$, is much smaller than the beam diameter and is determined by the laser optic system, where λ_0 is the laser wavelength in vacuum and F is the optic f -number (the ratio of the focal length of the lens divided by the lens diameter). We take $l_c = F\lambda_0/\pi$. Since there is always finite probability of obtaining such collapsing speckles in the random Gaussian field model, the beam angular divergence, $\Delta\theta$, increases with each collapse event. $\Delta\theta$ in vacuum is given by $\Delta\theta = 1/F$, for $F^2 \gg 1$. If the probability of speckle collapse is small, then the beam will keep its initial form. But if laser power is so large that power of many hot spots exceeds P_c then the beam will disintegrate into many small beams, leading to rapid change in $\Delta\theta$, (beam spray). Figures 1b and 1c show examples of both regime of strong and negligible beam spray.

An important measure of beam spray in this time independent regime is the fraction, $P_{scattered}$, of beam power, P_{beam} , in speckles which self-focus as the beam propagates, estimated as follows. NIF optic is approximately square, and hence a speckle area is $F^2\lambda_0^2$, implying a critical intensity for speckle self-focusing, $I_c = P_c/(F\lambda_0)^2 \approx 2 \times 10^{16} \text{W/cm}^2$.

The a priori probability distribution of speckle intensities implies that the mean number M of speckles (local maxima) in volume V with intensities above value I is given by (see Eq. (21) of Ref. [17])

$$M(I) = \frac{\pi^{3/2}\sqrt{5}V}{27F^4\lambda_0^3\pi} \left[\left(\frac{I}{\langle I \rangle} \right)^{3/2} - \frac{3}{10} \left(\frac{I}{\langle I \rangle} \right)^{1/2} \right] \exp \left(-\frac{I}{\langle I \rangle} \right), \quad (1)$$

where $\langle I \rangle = P_{beam}/S$ is the average beam intensity, S is the beam cross section. Then $M(I_c)$ is the number of collapses per volume V and $P_{scattered} = P_c M(I_c)$ is the optical power scattered out of the main beam due to self-focusing. Therefore, rate of scattering is given by

$$P_{beam}^{-1} dP_{scattered}/dz = \frac{P_c M(I_c)}{\langle I \rangle V}. \quad (2)$$

For NIF parameters, Eqs. (1) and (2) give $P_{beam}^{-1} dP_{scattered}/dz = 0.0002/\text{cm}$ for $\langle I \rangle = 10^{15} \text{W/cm}^2$ and $P_{beam}^{-1} dP_{scattered}/dz = 0.8/\text{cm}$ for $\langle I \rangle = 2 \times 10^{15} \text{W/cm}^2$. If Max's lower value of P_c were used, order unity of the total beam power would have been predicted to scatter

over a typical NIF plasma length of 1cm, even at the lower intensity since $dP_{scattered}/dz$ is exponentially sensitive (see Eq. (1)) to the parameter α , with $dP_{scattered}/dz \propto \exp(-\alpha)$, and $\alpha = I_c/\langle I \rangle$. For NIF parameters, $\alpha \gg 1$.

TIME-DEPENDENT SELF-FOCUSING

Clearly beam spray due to speckle self-focusing could be a problem at the higher intensity. This is alleviated by temporal beam smoothing techniques [18, 19] which induce finite speckle coherence time, T_c : the intensity distribution of light intensity inside plasma is given by a speckle field at each moment of time as in Figure 1a but location of hot spots changes in a random manner with a typical time T_c . Such techniques are used in contemporary experiments [8] and in future experiments at NIF.

Inertia weakens the plasma density response: if T_c is less than the duration of a particular self-focusing event, $\approx F\lambda_0/c_s\sqrt{P/P_c}$, (this estimate is accurate for $P/P_c \gtrsim 2.5$, see Ref. [15]) then this self-focusing event will be suppressed. This suppression effect is significant if $T_c \lesssim F\lambda_0/c_s$, i.e., T_c must be smaller than the time it takes for a sound wave to cross a speckle width (~ 4 ps for NIF parameters). Here c_s is the ion-acoustic wave speed. (This is in contrast to the case of almost instantaneous response of optical Kerr nonlinearity which is typical for solids [5]). As T_c decreases, a smaller fraction of the beam power participates in collapse events, controlled by the parameter $\alpha(l_c/c_s T_c)^2$, instead of α , for time independent self-focusing. This has led to the common assumption [4] that if the total power participating in independent collapse events is made arbitrarily small by reducing T_c , then beam spray could be reduced to any desired level.

However, we have found [7] that even for very small T_c , self-focusing can lead to strong beam spray. Now, self-focusing results from a collective instability, CFSBS, which couples the beam to ion acoustic waves that propagate transversely to the direction of laser beam propagation. As l_c increases, the well-known dispersion relation of forward stimulated Brillouin scattering [20] is recovered for coherent laser beam. We predict that this instability is not a sensitive function T_c for $c_s T_c \lesssim F\lambda_0$. Recent experiments at the Omega laser facility [8] are in excellent agreement with that prediction: It was found that reducing T_c from 3.4ps (for which $c_s T_c \approx F\lambda_0$) to 1.7ps did not cause a further reduction of beam spray at $\langle I \rangle = 5 \times 10^{14}$ W/cm². Note that dominant seed for CFSBS is not thermal but

time-dependent plasma density fluctuations caused by fluctuating speckles.

THERMAL SELF-FOCUSING

Quantitative comparison with this data requires extension of our earlier work [7] to allow transport of fluctuations, δT_e , in electron temperature. In that case the second mechanism of self-focusing - thermal self-focusing comes into play. Propagation of laser beam is described by paraxial equation for the electric field spatiotemporal envelope, E ,

$$\left(i\frac{\partial}{\partial z} + \frac{1}{2k_0}\nabla^2 - \frac{k_0 n_e}{2 n_c}\rho\right)E = 0, \quad \nabla = \left(\frac{\partial}{\partial x}, \frac{\partial}{\partial y}\right), \quad (3)$$

which is coupled to linearized hydrodynamic equation for the relative density fluctuation, $\rho = \delta n_e/n_e$, as it propagates acoustically with acoustic speed c_s :

$$\left(\frac{\partial^2}{\partial t^2} + 2\tilde{\nu}\frac{\partial}{\partial t} - c_s^2\nabla^2\right)\ln(1 + \rho) = c_s^2\nabla^2\left(I + \frac{\delta T_e}{T_e}\right), \quad (4)$$

where δT_e is the fluctuation of electron temperature, $k_0 = 2\pi/\lambda_0$, $I = |E|^2$ is the light intensity, $\tilde{\nu}$ is an integral operator whose Fourier transform in x and y is $\nu_{ia}k c_s$, where ν_{ia} is the ion acoustic wave amplitude damping rate normalized to the ion acoustic frequency. x and y are transverse directions to beam propagation direction z . E is in thermal units defined so that in equilibrium, with uniform E , the standard $\rho = \exp(-I) - 1$ is recovered. $n_c = m_e\omega_0^2/4\pi e^2$ is the critical electron density, m_e is the electron mass and e is the electron charge. The relative electron temperature fluctuation, $\delta T_e/T_e$ is responsible for thermal self-focusing and was omitted in our previous work [7].

We make the ansatz that the Fourier transform of electron temperature fluctuation, $\delta T_e(k)/T_e$ satisfies,

$$\left(\tau_{ib}\frac{\partial}{\partial t} + 1\right)\frac{\delta T_e(k)}{T_e} = g(k\lambda_e)I(k), \quad (5)$$

which is a reduced version of Epperlein's model [25]. Here the right-hand-side (r.h.s.) determines plasma heating by the inverse bremsstrahlung, $I(k)$ is the Fourier transform of I , so that intensity fluctuations are a source of δT_e [9]. The inverse bremsstrahlung relaxation time, τ_{ib} , is given by,

$$\tau_{ib} = \frac{1}{kc_s} \frac{3}{128} \sqrt{\frac{\pi Z^* \phi}{2}} \frac{[1 + (30k\lambda_e)^{4/3}]}{k\lambda_e} \frac{c_s}{v_e}. \quad (6)$$

Also

$$g(k\lambda_e) = \frac{[1 + (30k\lambda_e)^{4/3}]}{96(k\lambda_e)^2} Z^*, \quad (7)$$

and ϕ is an empirical factor [23], $\phi = (4.2 + Z^*)/(0.24 + Z^*)$, $Z^* = \sum_i n_i Z_i^2 / \sum_i n_i Z_i$ is the effective plasma ionization number, n_i and Z_i are the number density and the ionization number (number of ionized electrons per atom) of i -th ion species of plasma, respectively. λ_e is related to the standard $e - i$ mean free path, λ_{ei} , by $\lambda_e = (\lambda_{ei}/3)(2Z^*/\pi\phi)^{1/2}$. The basic ion acoustic wave parameters, ν_{ia} and c_s , are regarded as given by kinetic theory [27, 28, 29] which, e.g., takes into account the effect of compressional heating on sound wave propagation. For comparison with experiment in this paper, however, collisionless theory is used for evaluation of acoustic wave parameters.

Eq. (5) implies that thermal conductivity is determined by

$$\kappa = \frac{3}{2} \frac{n_e}{\tau_{ib} k^2} = \frac{k_{SH}}{1 + (30k\lambda_e)^{4/3}}, \quad (8)$$

where k_{SH} is the classical Spitzer-Harm [21] thermal conductivity coefficient in plasma. Since l_c is *not* small compared to the electron ion mean free path, λ_{ei} , thermal transport becomes nonlocal, and k_{SH} is effectively reduced, as given by Eq. (8), when applied to a fluctuation at speckle wavenumbers, $k = O(1/l_c)$. This reduction of κ_{SH} is substantial for experiment of Ref. [8], implying much larger δT_e than classical transport [25]. Importance of the thermal contribution to self-focusing at the speckle scale was first realized by Epperlein [22, 25], on the basis of Fokker-Planck simulations, and later analytically derived [24] and verified experimentally [26]. It was recently realized [27, 28] that Epperlein's result [22, 25] is correct provided the acoustic frequency c_s/l_c is smaller than the electron-ion collision frequency ν_e/λ_{ei} .

To solve Eqs. (3), (4) and (5) we need to determine boundary conditions on E . We assume, absent plasma, that in the optic far field the Fourier spectrum of E is top-hat with square shape:

$$|\hat{E}(\mathbf{k})| = \text{const for } |k_x| < k_m \text{ and } |k_y| < k_m; |\hat{E}(\mathbf{k})| = 0, \text{ otherwise,} \quad (9)$$

where $k_m = l_c^{-1}$. Thus our boundary conditions correspond to square top hat. The superposition of all these Fourier modes propagating in uniform density plasma we refer to as E_0 , the solution of Eq. (3) with $\rho = 0$. We assume temporal beam smoothing which means that

Fourier modes $\hat{E}(\mathbf{k})$ with different \mathbf{k} are uncorrelated and the modes with the same \mathbf{k} are correlated with short correlation time $T_c < l_c/c_s$.

For NIF designs, Z^* is highly variable depending on details of plasma composition. Laser beam may pass through, *e.g.*, *He*, *Be*, *CH*, *SiO₂* and *Au* plasma, allowing a wide range of Z^* . When Z^* is small, thermal effects are small, and our previous ponderomotive theory [7] applies. In this case, the linear stage of the collective instability depends only on one parameter - dimensionless intensity [7],

$$\tilde{I}_0 = \frac{4F^2}{\nu_{ia}} \frac{n_e}{n_c} I_0 \propto \frac{1}{\alpha \nu_{ia}}. \quad (10)$$

I_0 is the spatial average of $|E|^2$. Note that the standard figure of merit for self-focusing, $1/\alpha$, is smaller by the factor ν_{ia} (see Ref. [4]).

COLLECTIVE FORWARD STIMULATED BRILLOUIN SCATTER AND TRANSITION TO BEAM SPRAY REGIME

For small T_c , one might expect $\rho \simeq 0$ and that the laser beam would propagate with $E = E_0$. However, linearization of Eqs. (3), (4) and (5) about this state shows that this propagation is unstable. Following ideas of Ref. [7] and setting $\rho = \delta \rho e^{\lambda z} \exp[i(\mathbf{k} \cdot \mathbf{x} - \omega t)]$, $E = E_0 + \delta E e^{\lambda z} \exp[i(\mathbf{k} \cdot \mathbf{x} - \omega t)]$, we obtain the following dispersion relation, at acoustic resonance $\omega = kc_s$, assuming \mathbf{k} parallel to either the x or y directions:

$$2i\nu_{ia} = \left[1 - \frac{g(k\lambda_e)}{1 - ikc_s\tau_{ib}} \right] \frac{\delta I}{\delta \rho}, \quad (11)$$

where the plasma density response function $\delta I/\delta \rho$ is given by

$$\frac{\delta I}{\delta \rho} = \frac{n_e}{n_c} \frac{k_0^2 I_0}{4kk_m} \ln \frac{k^2(-2k_m + k)^2 + 4k_0^2\lambda^2}{k^2(2k_m + k)^2 + 4k_0^2\lambda^2}. \quad (12)$$

In general case of arbitrary direction of \mathbf{k} the dispersion relation is much more bulky and not given here because it gives essentially the same result.

Note that for $k_m \rightarrow 0$ ($F^2 \gg 1$) Eq. (12) reduces to

$$\frac{\delta I}{\delta \rho} = -\frac{n_e}{n_c} \frac{2k^2 k_0^2 I_0}{4k_0^2\lambda^2 + k^4} \quad (13)$$

which means that Eq. (11), absent thermal effects (i.e. for $\delta T_e = 0$ in Eq. ((4)), reduces to the paraxial limit of the standard FSBS dispersion relation [20].

Absent thermal effects we regain the ponderomotive case considered in Ref. [7] except that in this Article square top hat boundary conditions (9) are used compared with circular top hat boundary conditions used in [7]. We find however that both circular and square top hat boundary conditions give similar results.

Positive value of $Re(\lambda)$ corresponds to convective instability so that the fluctuations of beam intensity grow as $\exp[Re(\lambda)z]$ with distance. When λ is non-dimensionalized, $\tilde{\lambda} = l_c^2 k_0 \lambda$, it only depends on

$$\tilde{I} \equiv \left[1 + \frac{g(k\lambda_e)}{1 - ikc_s\tau_{ib}} \right] \tilde{I}_0. \quad (14)$$

Here k is determined from the condition that $Re(\lambda)$ is maximum and \tilde{I}_0 is given by (10). According to our theory of CFSBS, λ^{-1} , should be compared with the basic correlation length in z direction, known as the speckle length, $l_{speckle} \approx 7F^2\lambda_0$. The value $\tilde{\lambda} = 0.1$, at which $\lambda \approx l_{speckle}$, marks regime transition. In the first, weak regime, with $\tilde{\lambda} \ll 0.1$, there is little gain over a speckle length. It follows that only small changes in correlations develop over a speckle length, in particular, there is little change in $\Delta\theta$. Changes over different speckles are uncorrelated, leading to a quasi-equilibrium (see Figure 3 of Ref. [7]). As $\tilde{\lambda}$ crosses the value 0.1 (corresponding to $\tilde{I} \approx 2$ in ponderomotive case), a second, non-equilibrium regime, is entered, and beam properties change rapidly with z . In particular, $\Delta\theta$ changes rapidly, *i.e.*, there is beam spray. This is shown in Figure 2, where normalized beam spray rate is shown. Note that absent instability one expects beam spray rate $d\langle\theta^2\rangle/dz \sim I_0^2$. So in Figure 2 we normalized beam spray rate to I_0^2 (see Ref. [7] for more discussion). Compared with Figure 6 of Ref. [7], there has been an important change of independent variable, from \tilde{I} to $\tilde{\lambda}$, which allows a unified presentation of both ponderomotive and thermal cases.

Thus analysis of $\tilde{\lambda}$ results in second and main conclusion of our CFSBS theory: prediction of the onset of beam spray, and hence a prediction of fundamental limit on power propagation. Here we present comparison of this prediction with [8], the first experimental measurement of beam spray onset (see Figure 3). From [8, 30, 31] we find that $0.14 < n_e/n_c < 0.25$. $T_e \sim 2\text{keV}$, $F = 6.7$, $\omega_0 \approx 3.6 \times 10^{15}\text{sec}^{-1}$, and $Z^* = 6.4$ at upper range of densities. For a nominal electron density of $n_e = 0.2n_c$, the 0.1 contour (color online) of $\tilde{\lambda}$ is shown in Figure 4a, implying $\tilde{I} \approx 0.65$ at regime transition. was observed [8], corresponds to $\tilde{I} \approx 1.05$, with Landau damping $\nu_{ia} = 0.06$ for the plasma composition at this density. The major uncertainty in comparing this data with theory is due to significant

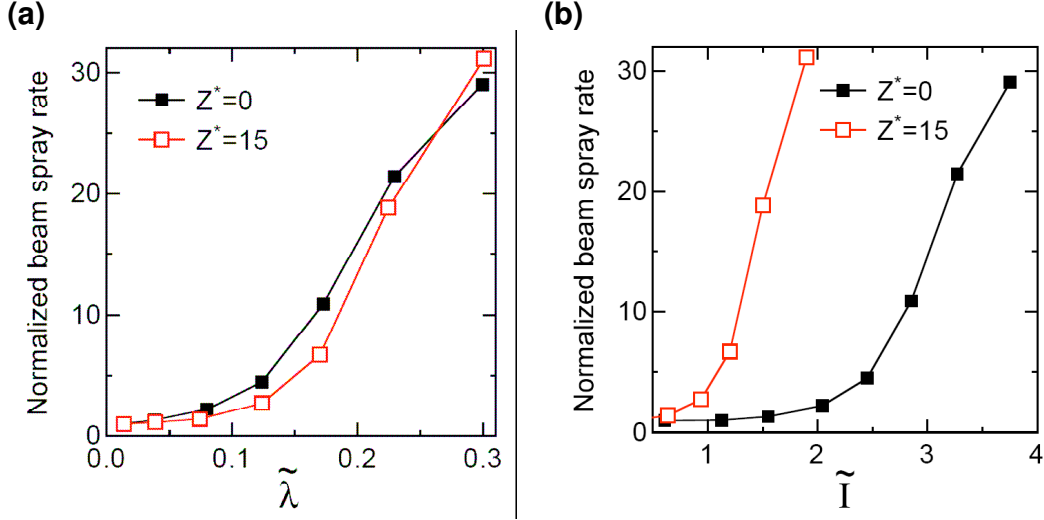


FIG. 2: Figure 2. Dependence of beam spray rate obtained from simulations as a function of (a) dimensionless growth rate $\tilde{\lambda}$ and (b) dimensionless intensity \tilde{I} . Red curves correspond to ponderomotive self-focusing ($Z^* = 0$) and black curves ($Z^* = 15$) correspond to case where both ponderomotive and thermal self-focusing are essential. Both red and black curves collapse to the single curve in (a) which indicated that $\tilde{\lambda}$ is a much better parameter for onset of beam spray, compared with \tilde{I} .

time dependence of T_e/T_i during experiments as well as plasma density inhomogeneity, *e.g.*, if $n_e = 0.14n_c$ (which corresponds to plasma density plateau in Figure 3 of Ref. [8]) with other parameters the same, then theory predicts $\tilde{I} \approx 0.73$ and experiments give $\tilde{I} \approx 0.82$. In contrast, prediction based on speckle collapses, gives that even at the maximum density of $n_e/n_c = 0.25$, $P_{beam}^{-1} dP_{scattered}/dz = 0.23\text{cm}^{-1}$, the scattered power fraction, $P_{scattered}/P_{beam}$, is only 0.5% after $200\mu\text{m}$ of propagation through the high-density region of the plasma. This is much less than the observed [8] 10%. Therefore, beam spray due to CFSBS is consistent with the data while beam spray due to speckle collapse is not.

IMPLICATION FOR BACKSCATTERING

Recent experiments at the Atomic Weapon Establishment in the UK have demonstrated reduction of both stimulated Brillouin and Raman backscatter [32] by the addition of small amounts of high ionization state dopants to a low ionization state plasma, *e.g.*, a 1% dopant

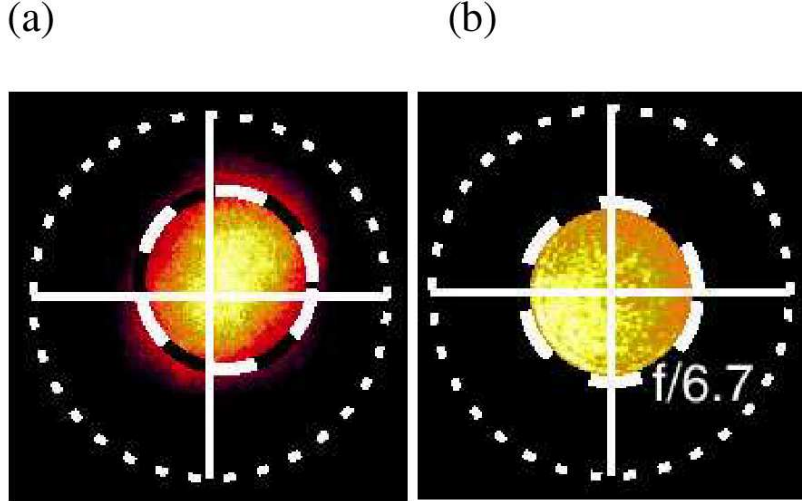


Figure 3

FIG. 3: Figure 3. Experimental images of cross section of time averaged laser beam intensity after propagation through plasma. (a) Onset of beam spray regime at $5 \times 10^{14} \text{W/cm}^2$. (b) Negligible beam spray regime achieved by lowering intensity. Dashed circles correspond to $F = 6.7$ beam width for propagation in vacuum. Reproduced from [8] with permission.

reduced backscatter by more than an order of magnitude. Combination of these experimental facts with our prediction that dopant may cause transition to beam spray regime suggests that one should expect anti-correlation between beam spray and backscatter. If this anti-correlation is confirmed experimentally then we propose the following mechanism: beam spray decreases speckle length (correlation length) with beam propagation and backscatter is suppressed by reduction of laser beam correlation length. The latter has been established through simulation [13], experiment [33] and one dimensional analytic theory [34]. In other words, control of backscatter is achieved indirectly through control of CFSBS. We are unaware of any other explanation of this backscatter reduction by the addition of small amounts of high Z dopant.

Clearly, to maintain control of forward beam propagation, beam spray must not be strong. If plasma parameters are conducive to backscatter as in the Atomic Weapon Establishment experiment [32], then by altering the plasma state so as to be above, but close to, the beam spray regime transition, allowing moderate beam spray might lead to optimum control of

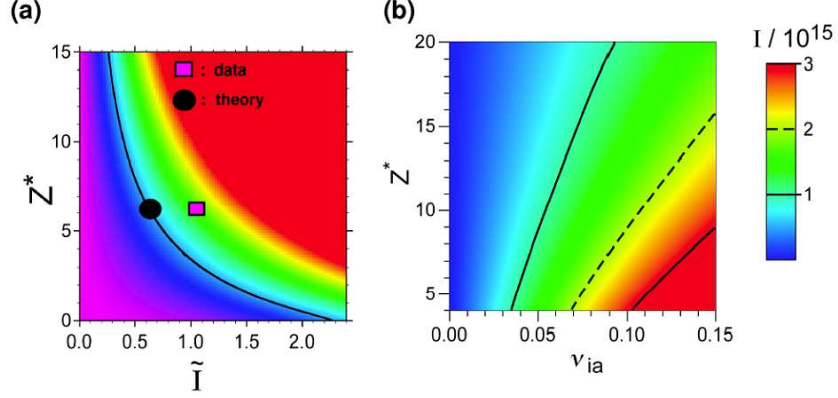


FIG. 4: Figure 4. (a) Solid curve separates predicted beam spray regime, $\tilde{\lambda} > 0.1$ (from green to red colours), from negligible beam spray regime $\tilde{\lambda} < 0.1$, (from blue to purple colours). Different colours denote values of $\tilde{\lambda}$, with red corresponding to the value 0.3 and above. Magenta square denotes experimentally measured (Ref. [8]) beam spray onset, assuming $\nu_{ia} = 0.06$ and black circle is the theoretical prediction for $\nu_{ia} = 0.06$. (b) Predicted onset of beam spray regime (*i.e.* for $\tilde{\lambda} = 0.1$) as a function of Z^* and ν_{ia} for NIF plasma with $T_e \sim 5\text{keV}$, $F = 8$, $n_e/n_c = 0.1$, $\omega_0 \approx 5.4 \times 10^{15}\text{sec}^{-1}$. Colours show laser intensity, in units of 10^{15}W/cm^2 . Intensity is at maximum for small Z^* and large ν_{ia} . We assume $Z^* > 4$ to make sure that condition $c_s/l_c < v_e/\lambda_{ei}$ is true.

beam propagation and backscatter. This suggests operating above but, *e.g.*, close to the solid curve of figure 4a which marks the transition regime of CFSBS.

CONCLUSION

In conclusion, transition to the beam spray regime was recognized as a collective phenomenon. Our theory is in excellent agreement with experiment: the transition laser intensity and its insensitivity to changes in correlation time were predicted. We found that the growth rate of CFSBS depends on four dimensionless parameters: the scaled laser intensity \tilde{I}_0 (see Eq. (10)), scaled electron-ion mean free path $\lambda_{ei}/F\lambda_0$, effective ionization number Z^* , and c_s/v_e . The first three of these can be manipulated experimentally. So our theory permits predictions for beam control at NIF that may be implemented since thermal self-focusing can be manipulated experimentally through control of CFSBS in two ways. First, by changing Z^* through change of plasma composition. For example, addition of 1% of

Xenon (high Z dopant) to low Z plasma (50% of He and 50% of H) would increase Z^* from 1.7 to 15.5 without significant change in ν_{ia} . Second, beam control can be implemented by adding low Z dopant to a high Z plasma, e.g., adding He to SiO_2 , in order to increase ν_{ia} at almost constant Z^* . Figure 4b shows dependence of laser intensity (indicated by colors) at predicted onset of beam spray regime on Z^* and ν_{ia} for NIF parameters. It is seen that maximal allowable intensity occurs for small Z^* and large ν_{ia} . We propose Figure 4b as direct guide for choice of NIF designs to attain maximum power of laser beam, which may propagate without significant beam spray.

Observation of anti-correlation between beam spray and backscatter, through the addition of small amounts of high Z dopant, would mean additional confirmation of our theory. We predict that control of backscatter is achieved indirectly through control of CFSBS, e.g. by changing plasma ionization state and/or acoustic damping [35].

Acknowledgements We thank R.L. Berger for attracting our attention to Refs. [27, 28] and pointing out that seed for CFSBS provided by the fluctuating speckles is much larger than thermal. We thank W. Rozmus for pointing out the limitation of Epperlein's model [22, 25] to $c_s/l_c < v_e/\lambda_{ei}$. Support was provided by the Department of Energy, under contract W-7405-ENG-36.

Correspondence and requests for materials should be addressed to H.R. (har@lanl.gov).

* Electronic address: har@lanl.gov

- [1] McCrory R L et. al. 1988 Nature **335** 225
- [2] Still C H et al. 2000 Physics of Plasmas **7** 2023
- [3] Miller G H Moses E I & Wuest C R 2004 Nucl. Fusion **44** S228
- [4] Lindl J D et. al. 2004 Phys. Plasmas **11**, 339
- [5] Boyd RW 2002 Nonlinear Optics (Academic Press, San Diego)
- [6] Sulem C and Sulem P L 1999 Nonlinear Schroedinger Equations: Self-Focusing and Wave Collapse (Springer)
- [7] Lushnikov P M and Rose H A 2004 Phys. Rev. Lett. **92** 255003
- [8] Niemann C et. al., 2005 Phys. Rev. Lett. **94** 085005
- [9] Kruer W L 1990 The physics of laser plasma interactions. Addison-Wesley, New York)

- [10] Zakharov V E and Shabat A B 1971 Zh. Eksp. Teor. Fiz., **61** 118 [1972 Sov. Phys. JETP, **34**, 62]
- [11] Chiao R Y, Garmire E and Townes C H 1964 Phys. Rev. Lett. **13** 479
- [12] Talanov V I 1965 JETP Letters **2** 138
- [13] Rose H A and DuBois D F 1994 Phys. Rev. Lett. **72** 2883-2886
- [14] Max C E 1976 Phys. Fluids **19** 74
- [15] Rose H A and DuBois D 1993 Phys. Fluids B **5** 3337
- [16] Kato Y and Mima K 1982 Appl. Phys. B **29** 186
- [17] Garnier J 1999 Phys. Plasmas **6** 1601 Eq. (21).
- [18] Lehmburg R H and Obenschain S P 1983 Opt. Commun. **46** 27
- [19] Skupsky S et. al., 1989 J. Appl. Phys. **66** 3456
- [20] Schmitt A J and Afeyan B B 1998 Phys. Plasmas **5** 503
- [21] Spitzer L Jr and Harm R 1953 Phys. Rev. **89** 977
- [22] Epperlein E M 1990 Phys. Rev. Lett. **65** 2145
- [23] Epperlein E M and Short R W 1992 Phys. Fluids **B4**, 2211
- [24] Maximov AV and Silin V P 1993 Zh. Eksp. Teor. Fiz., **103** 73 [1993 Sov. Phys. JETP **76** 39]
- [25] Epperlein E M and Short R W 1994 Phys. Plasmas. **1** 3003
- [26] Montgomery D S, Johnson R P, Rose H A, Cobble J A and Fernandez J C 2000 Phys. Rev. Lett. **84** 678
- [27] Brantov A V et. al., 2004 Phys. Rev. Lett. **93** 125002
- [28] Berger R L, Valeo E J, and Brunner S 2005 Phys. Plasmas **12** 062508
- [29] Berger R L, and Valeo E J 2005 Phys. Plasmas **12** 032104
- [30] We thank C. Niemann for communicating to us the detailed plasma composition.
- [31] Determined by simulation, results provided by N.B. Meezan, private comm. (2005)
- [32] Suter L J et. al. 2004 Phys. Plasmas **11** 2738
- [33] Fernandez J C et. al. 1996 Phys. Rev. E **53** 2747
- [34] Mounaix Ph. 1995 Phys. Plasmas **2** 1804
- [35] Reduction of Stimulated Raman backscatter by reducing acoustic damping has been observed in Fernandez J C et. al. 1997 Phys. Plasm. **4** 1849